GLEMSER, O., HOLZNAGEL, W. & ALI, S. I. (1965). *Z. Naturforsch. Teil B*, **20**, 192–199.
GLEMSER, O., HOLZNAGEL, W., HÖLTJE, W. & SCHWARZMANN, E. (1965). *Z. Naturforsch. Teil B*, **20**, 725–746.
GLEMSER, O. & TYTKO, K.-H. (1969). *Z. Naturforsch. Teil B*, **24**, 648.
GLEMSER, O., WAGNER, G., KREBS, B. & TYTKO, K.-H. (1970). *Angew. Chem.* **82**, 639; *Angew. Chem. Int. Ed. Engl.* **9**, 639.
HEDMAN, B. & STRANDBERG, R. (1978). Personal communication.
International Tables for X-ray Crystallography (1974). Vol. IV, pp. 99 ff. Birmingham: Kynoch Press.
ISOBE, M., MARUMO, F., YAMASE, T. & IKAWA, T. (1978). *Acta Cryst.* B**34**, 2728–2731.
JANDER, G., JAHR, K. F. & HEUKESHOVEN, W. (1930). *Z. Anorg. Allg. Chem.* **194**, 383–428.
KIHLBORG, L. (1960). *Acta Chem. Scand.* **14**, 1612–1622.
KIHLBORG, L. (1963). *Ark. Kemi*, **21**, 427–437.
KNÖPNADEL, I., HARTL, H., HUNNIUS, W.-D. & FUCHS, J. (1974). *Angew. Chem.* **86**, 894–895; *Angew. Chem. Int. Ed. Engl.* **13**, 823–824.
KREBS, B. (1969). *Acta Cryst.* A**25**, S104.
KREBS, B. (1970). *J. Chem. Soc. Chem. Commun.* pp. 50–51.
KREBS, B. (1972). *Acta Cryst.* B**28**, 2222–2231.
KREBS, B. & PAULAT-BÖSCHEN, I. (1976). *Acta Cryst.* B**32**, 1697–1704.
KREBS, B. & PAULAT-BÖSCHEN, I. (1979). 5th Eur. Crystallogr. Meet., Copenhagen, Abstracts, p. 245.
KWAK, W., RAJKOVIĆ, L. M., POPE, M. T., QUICKSALL, C. O., MATSUMOTO, K. Y. & SASAKI, Y. (1977). *J. Am. Chem. Soc.* **99**, 6463–6464.
LINDQVIST, I. (1950*a*). *Ark. Kemi*, **2**, 325–341.
LINDQVIST, I. (1950*b*). *Ark. Kemi*, **2**, 349–355.
MATSUMOTO, K. Y. (1978). *Bull. Chem. Soc. Jpn*, **51**, 492–498.
OSWALD, H. R., GÜNTER, J. R. & DUBLER, E. (1975). *J. Solid State Chem.* **13**, 330–338.
PAULAT-BÖSCHEN, I. (1979). *J. Chem. Soc. Chem. Commun.* pp. 780–782.
PAULING, L. (1947). *J. Am. Chem. Soc.* **69**, 542–553.
SASAKI, Y. & SILLÉN, L. G. (1968). *Ark. Kemi*, **29**, 253–277.
SCHRÖDER, F. A. (1975). *Acta Cryst.* B**31**, 2294–2309.
SHELDRICK, G. M. (1979). *SHELXTL*. Structure determination system. Univ. of Cambridge, England.
SJÖBOM, K. & HEDMAN, B. (1973). *Acta Chem. Scand.* **27**, 3673–3691.
Syntex *EXTL* (1976). Program system for structure determination, Syntex Analytical Instruments Ltd., Cupertino, California.
TYTKO, K.-H. & GLEMSER, O. (1970). *Z. Naturforsch. Teil B*, **25**, 429–430.
TYTKO, K.-H. & GLEMSER, O. (1976). *Adv. Inorg. Chem. Radiochem.* **19**, 239–315.
TYTKO, K.-H. & SCHÖNFELD, B. (1975). *Z. Naturforsch. Teil B*, **30**, 471–484.
TYTKO, K.-H., SCHÖNFELD, B., BUSS, B. & GLEMSER, O. (1973). *Angew. Chem.* **85**, 305–307; *Angew. Chem. Int. Ed. Engl.* **12**, 330–332.
VIVIER, H., BERNARD, J. & DJOMAA, H. (1977). *Rev. Chim. Minér.* **14**, 584–604.

Acta Cryst. (1982). B**38**, 1718–1723

The Structure of Magnetite: Defect Structure II

BY MICHAEL E. FLEET

Department of Geology, University of Western Ontario, London, Ontario, Canada N6A 5B7

(*Received* 5 *November* 1981; *accepted* 14 *January* 1982)

Abstract

$Mg_{0.04}Fe_{2.96}O_4$ is cubic, *Fd3m*, with $a = 8{\cdot}3930\ (6)$ Å. The structure of magnetite from a skarn-type iron-ore deposit has been refined to a weighted R of 0·024 using 145 unique averaged reflections collected at room temperature on a single-crystal diffractometer with Mo $K\alpha$ ($\lambda = 0{\cdot}7107$ Å) radiation. The oxygen positional parameter (u) is 0·2547 (1). Residual electron density peaks at equipoint positions 48(f) and 96(h) have been assigned, respectively, to interstitial Fe^{3+} in a second tetrahedrally coordinated position and to interstitial Fe^{2+}, Fe^{3+} in a second octahedrally coordinated position. Corresponding vacancies are present in the tetrahedral and octahedral cation positions of the ideal inverse-spinel structure: Fe, Mg occupancies for these positions are 0·93 and 0·95, respectively. Weak $\langle 110 \rangle^*$ diffraction streaks are attributed to lattice strain associated with the high concentration of point defects. This defect structure is basically different from that reported earlier for essentially 'pure' Fe_3O_4 from a different mineral paragenesis (chlorite schist).

Introduction

Magnetite has the inverse-spinel structure, with space group *Fd3m* (No. 227) and ideal structural formula TM_2O_4, where T is Fe^{3+} in tetrahedral coordination with oxygen and M is Fe^{3+} and Fe^{2+} in octahedral

0567-7408/82/061718-06$01.00

Table 1. *Occupancy, positional and thermal parameters for two refined magnetite structures*

Origin at centre ($\bar{3}m$). I is defect structure I, magnetite 633 (Fleet, 1981*a*): II is defect structure II, magnetite 2741. Thermal parameters ($\times 10^3$ Å^2) are calculated from $T = \exp\{-\frac{1}{4}[B_{11}a^{*2}(h^2 + k^2 + l^2) + 2B_{12}a^{*2}(hk + kl + hl)]\}$.

		Equipoint	Occupancy	x	y	z	B_{11}	B_{12}
I	$T(1)$	8(*a*)	1·024 (26)	$\frac{1}{8}$	$\frac{1}{8}$	$\frac{1}{8}$	344 (17)	
	$M(1)$	16(*d*)	1·017 (26)	$\frac{1}{2}$	$\frac{1}{2}$	$\frac{1}{2}$	453 (14)	46 (5)
	O	32(*e*)	1·0	0·2549 (1)	0·2549 (1)	0·2549 (1)	509 (44)	3 (17)
	$T(2)$	8(*b*)	0·010 (4)	$\frac{3}{8}$	$\frac{3}{8}$	$\frac{3}{8}$	$T(1)$	
II	$T(1)$	8(*a*)	0·918 (14) Mg, 0·013	$\frac{1}{8}$	$\frac{1}{8}$	$\frac{1}{8}$	342 (17)	
	$M(1)$	16(*d*)	0·940 (12) Mg, 0·013	$\frac{1}{2}$	$\frac{1}{2}$	$\frac{1}{2}$	456 (12)	27 (5)
	O	32(*e*)	1·0	0·2547 (1)	0·2547 (1)	0·2547 (1)	594 (30)	83 (20)
	$T(3)$	48(*f*)	0·010 (1)	0·375	$\frac{1}{8}$	$\frac{1}{8}$	$T(1)$	
	$M(2)$	96(*h*)	0·007 (1)	0	0·0179 (14)	0·9821 (14)	$M(1)$	

coordination. A recent high-resolution X-ray refinement of the crystal structure of a natural magnetite (No. 633; Fleet, 1981*a*) has demonstrated that the M—O bond distance and electron density distribution in the vicinity of the O atom are consistent with a common Fe^{3+} nucleus for M-site atoms as predicted by modern theories on the electronic structure of magnetite. Furthermore weak residual electron density at equipoint position 8(*b*) was assigned to interstitial Fe^{3+} in a second tetrahedrally coordinated position, $T(2)$. It was surmised that the structure of magnetite 633 has corresponding vacancies in $M(1)$ sites adjacent to the occupied $T(2)$ sites forming an interstitial-vacancy couple similar to that reported for the defect structure of $Fe_{1-x}O$ (Roth, 1960). The refinement of this structure has now been extended to include cation site occupancies and the final parameters are included in Table 1. This crystal structure will be referred to provisionally as defect structure I.

The existence of interstitial Fe^{3+} in the $T(2)$ cation site of structure I is based on the following evidence: (1) the cation site occupancy refines to a value which is consistent with electron density peaks in both F_o and $F_o - F_c$ maps; (2) occupancy of $T(2)$ reduces the weighted and conventional residual indices; and (3) residual electron density at equipoint positions 96(*g*), 96(*h*) and 32(*e*) is consistent with the local displacements of $T(1)$, O and $M(1)$ atoms required when $T(2)$ is occupied. Clearly, the residual electron density at equipoint 8(*b*) is not an artifact of the structure refinement.

The present paper reports on a structure analysis of a second natural magnetite (No. 2741), which differs in both mineral paragenesis and composition from magnetite 633 and which, on the basis of preliminary single-crystal diffraction study (Fleet, 1981*a*), was suspected of having a crystal structure with a higher proportion of point defects than defect structure I.

Experimental

The sample of magnetite investigated in the present study (No. 2741, Dana Collection, University of Western Ontario) was from Iron County, Utah, a well-known locality for large magnetite octahedra (Sinkankas, 1964) within the Iron Springs iron-ore-deposits district. Iron-ore bodies of the Iron Springs district are skarn-like replacement deposits of magnetite and hematite in Jurassic limestone (Mackin, 1968). The hand specimen of 2741 consists of massive, drussy-like magnetite encrusted with magnetite octahedra and minor calcite and quartz. Coarse-grain surfaces of massive magnetite are striated in the manner of the striated dodecahedron {110} (*e.g.* Sinkankas, 1964). Striated surfaces frequently terminate in {111} faces and are evidently a parallel-growth feature. Hematite is present as a minor replacement (oxidation) product. In polished section it occurs as small irregular patches adjacent to fractures.

Extensive electron microprobe analysis indicated a composition of 0·69 wt% MgO, 93·14 wt% FeO, or $Mg_{0.039}Fe_{2.961}O_4$, using orthopyroxene (Mg) and essentially 'pure' natural magnetite (Fe) as standards. Si, Al, Ti, Cr, Mn, and Ca were analyzed for but not detected. Least-squares refinement of 12 centered high-angle reflections measured on a four-circle diffractometer with graphite-monochromatized Mo $K\alpha_1$ (λ = 0·70926 Å) radiation gave a = 8·3930 (6) Å, which is in good agreement with published data for Fe_3O_4 composition (Lindsley, 1976). Observed reflections of magnetite on precession and Weissenberg films are consistent with space group $Fd\bar{3}m$. Sporadic very weak $hk0$ reflections with $h + k = 4n + 2$ were confirmed as multiple reflections (Samuelsen, 1974) by varying the conditions of diffraction (*e.g.* on a-axis Weissenberg films using unfiltered Cr radiation only the $K\beta$ 420 reflection is observed). Diffuse diffraction streaks are

associated with some of the stronger reflections: these will be discussed more fully below.

Other weak reflections on precession films are due to oriented inclusions of hematite. The orientation relationship of the hematite and magnetite reciprocal lattices is that expected for topotaxic replacement with minimal reorganization of the {111} close-packed oxygen layers in the magnetite structure, $c_{hm} \| [111]_{mt}$; $a_{hm} \| [\bar{1}\bar{1}2]_{mt}$. Four out of every six oxygen layers in magnetite do have to be reorganized (or shuffled) in the replacement, as is evident by comparison of schematic close-packed stacking sequences in the two structures:

magnetite	*CB AC BA CB AC BA*...
hematite	*CB CB CB CB CB CB*...

24 symmetry-equivalent hematite orientations are possible, but only a few of these are observed within the crystal volume normally used in X-ray diffraction studies.

The crystal selected for the structure refinement was an approximately equidimensional, trigonal prismatic-shaped single-crystal fragment, with a calculated volume of $1{\cdot}6 \times 10^{-3}$ mm^3, which had been trimmed to remove parts with oriented hematite inclusions. The X-ray intensity data were collected at room temperature on a Picker FACS-1 four-circle diffractometer system by the θ–2θ scan technique: 40 s stationary background counts, peak-base widths of 2° 2θ and a scanning rate of 2° min^{-1}. All hkl and $\bar{h}k\bar{l}$ reflections with $h + k$, $k + l$, $l + h = 2n$ out to $2\theta = 90°$ were measured. The resulting data were processed with program *DATAP* 77 (SUNY at Buffalo) and corrected for background, Lorentz and polarization effects, and absorption. Transmission factors for the absorption correction were calculated by Gaussian integration with a 12 × 12 × 12 grid using a linear absorption coefficient of 14·65 mm^{-1}. The crystal was oriented with [110] parallel to the φ axis. The calculated transmission factors varied from 0·184 for $\bar{1}1\bar{1}$ to 0·326 for 11,11,5. The original list of 2574 reflections was reduced to 145 reflections non-equivalent in $Fd3m$. Standard deviations were calculated from the agreement between equivalent reflections. Zero intensity was assigned if more than 25% of a set of equivalent reflections had peak intensities less than background plus one standard deviation.

Diffuse X-ray diffraction streaks

Certain X-ray reflections of magnetite 2741 exhibit a slight asterism. The affected reflections are misshaped with puckered perimeters which extend into diffuse diffraction streaks. Asterism is most prominent in [110] precession films (Fig. 1), and is preferentially, but not exclusively, associated with the strongest reflections

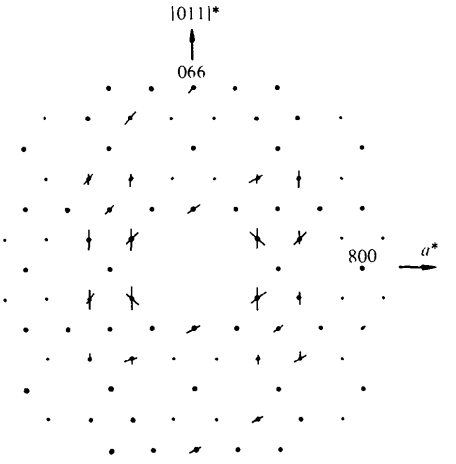

Fig. 1. Representation of zero-layer, |01̄1|-axis precession photograph of magnetite 2741, showing distribution of diffuse diffraction streaks: Mo $K\alpha$ radiation, $\mu = 25°$.

(311, 511, 220, 333, 555, *etc.*). The only class of $Fd3m$ reflections which does not exhibit asterism seems to be $h00$. Most frequently the diffraction-streak intensity is proportional to the intensity of the associated Bragg reflection. It is emphasized however that the diffraction streaks represent only a very small proportion of the total coherent X-ray scattering, and exposures of 3 to 7 days with unfiltered radiation are normally required to resolve them properly.

Most of the diffraction streaks in |110| precession films (Fig. 1), and certainly all the stronger ones, are in one of three orientations; |011|*, ~|211|*, and ~|2̄11|*. The two latter orientations are irrational with respect to the reciprocal lattice of magnetite, and closer observation reveals that the orientation of individual streaks in any one set undergoes a progressive rotation across the diffraction pattern. The most logical explanation of this phenomenon is that the streaks with ~|211|* and ~|2̄11|* orientations actually belong to two other ⟨110⟩* orientations which are inclined to the plane of diffraction but nevertheless fall within the annular slit of the layer-line screen. The mean observed streak orientations are approximately consistent with this interpretation.

A one-dimensional diffraction effect is logically interpreted in terms of a planar structural feature in the plane normal to the diffraction effect (Fleet, 1976, 1981*b*). Such planar structural features include stacking faults, twin lamellae, structural modulations and lamella precipitates. Thus diffuse continuous streaks in ⟨110⟩* directions indicate the presence in crystals of magnetite 2741 of a nonperiodic planar feature parallel to {110}. This orientation is inconsistent with any association of the diffraction streaks with submicroscopic hematite precipitates, (111) twin lamellae and dodecahedral {110} striations. Lamellar hematite

precipitates or intergrowths with magnetite should have a {111} morphology and, in any case, the asterism is unrelated to the presence or absence of oriented reflections of hematite. {110} planes are inappropriately oriented to produce the striations on dodecahedral faces, which are parallel to octahedral edges. The {110} striations are occasionally interpreted as the traces of (111) twin planes, especially in elementary textbooks. However, neither ⟨111⟩* streaks, indicative of coherent twinning, nor additional reflections, indicative of incoherent twinning, have been observed in extensive investigations of magnetite (and other spinel minerals) from a variety of different localities. Furthermore any of the possible (111) composition planes results in a twin structure quite different from that of magnetite.

Thus the nonperiodic planar feature responsible for the ⟨110⟩* diffraction streaks is possibly {110} stacking faults, a structural modulation, or some other form of lattice strain. {110} stacking faults seem energetically unfavorable. On the other hand the deformed Bragg reflections are consistent with lattice strain. This may be correlated with the high concentration of point defects resolved in the structure analysis (below). The lattice strain could arise either directly from the thermal relaxation of the defected structure or indirectly from incipient ordering of the point defects. Perhaps subsequent high-resolution transmission electron microscopy work will help to clarify this problem. Magnetostriction was considered as a possible source of lattice strain. However, the asterism is unaffected by demagnetization in an alternating-field demagnetizer of the type commonly used in palaeomagnetic studies.

Structure refinement

The crystal structure of magnetite 2741 was refined in space group $Fd3m$ using program *LINEX* 77 (SUNY at Buffalo). Initial structural parameters were those for the $T(1)$, $M(1)$ and O positions of magnetite 633 (defect structure I; Fleet, 1981*a*). Mg was assigned wholly to $T(1)$. Although the magnesioferrite end-member composition ($MgFe_2O_4$) does have a largely inverse structure (Kriessman & Harrison, 1956), there seemed to be at the outset of the present study no basis for estimating the octahedral site preference of minor amounts of Mg in magnetite. Therefore, the tetrahedral site preference observed on other spinel minerals (Osborne, Fleet & Bancroft, 1981) was assumed as a working hypothesis. Scattering curves for the neutral atomic species, and real and imaginary components of the anomalous-dispersion corrections were taken, respectively, from Tables 2.2*B* and 2.3.1 of *International Tables for X-ray Crystallography* (1974). The refinement with anisotropic thermal parameters for $M(1)$ and O and isotropic extinction converged on values for the weighted and conventional residual indices (R) of 0·036 and 0·047, respectively. Equivalent data for refinement with isotropic thermal parameters are 0·039 and 0·050, respectively.

Table 2. *Residual electron density peaks after refinement of ideal magnetite structure*

Equipoint position	x	y	z	Relative electron density (%)*
16(c)	0	0	0	3·3
48(f)	0·375	$\frac{1}{8}$	$\frac{1}{8}$	1·6

* Relative electron density is percentage of peak F_o electron density at $T(1)$ position.

At this stage in the refinement weak residual electron density peaks were observed in $F_o - F_c$ maps (Table 2). The most prominent residual electron density, that in the 16(c) equipoint position, was tentatively assigned to a second octahedrally coordinated cation position, $M(2)$, with an occupancy of 0·033. The addition of iron in $M(2)$ and cation vacancies in $M(1)$ to the structure reduced the weighted R to 0·029. The improved resolution on $F_o - F_c$ maps now showed the $M(2)$ cation to be in equipoint 96(h) with $x \sim 0{\cdot}020$. Residual electron density at 48(f) equipoint position (Table 2) was tentatively assigned to a second tetrahedrally coordinated cation position $T(3)$, with an occupancy of 0·016 [the '$T(2)$' label is already in use in the description of defect structure I]. The addition of iron in $T(3)$ and unconstrained $T(1)$, $M(1)$, $M(2)$ and $T(3)$ occupancies to the structure further reduced the weighted R to 0·024. The refined parameters included scale, O and $M(2)$ positions, $M(1)$ and O anisotropic thermal and isotropic extinction. $T(3)$ and $M(2)$ thermal parameters were constrained equal to those of $T(1)$ and $M(1)$, respectively.

The small proportion of Mg present in the structure was originally considered to have an insignificant effect on the refinement. Nevertheless several models for the structural location of Mg were included in the final stage of refinement (Table 3). On the basis of minimization of residual index *and* agreement of the total tetrahedral and octahedral cations with the stoichiometric values, Mg preferentially occupies $M(1)$ (models 3, 4 and 5). Model 4, with Mg in both $M(1)$ and $T(1)$, has been adopted as the final structure. However, this model is not statistically better than model 2 with Mg restricted to $M(1)$. It is also possible that Mg populates $T(3)$ and $M(2)$, as well as $M(1)$ and $T(1)$. However, the finite resolution of the present data set did not permit further site-occupancy refinement of $T(3)$ and $M(2)$.

Table 3. *Refinement of models for structural location of* Mg

Model*	1	2	3	4	5
Cation occupancy					
$T(1)$,Fe	0·906 (14)	0·925 (14)	0·912 (14)	0·918 (14)	0·918 (14)
$T(1)$,Mg	0·039	–	0·025	0·013	0·013
$T(3)$,Fe	0·062 (8)	0·062 (8)	0·062 (8)	0·062 (8)	0·062 (8)
Total	1·007 (16)	0·987 (16)	0·999 (16)	0·993 (16)	0·993 (16)
$M(1)$,Fe	1·892 (25)	1·873 (25)	1·885 (25)	1·879 (24)	1·879 (25)
$M(1)$,Mg	–	0·039	0·014	0·026	0·026
$M(2)$,Fe	0·085 (10)	0·085 (9)	0·085 (9)	0·085 (9)	0·085 (9)
Total	1·977 (27)	1·997 (27)	1·984 (27)	1·990 (26)	1·990 (27)
Residual indices†					
Rconv,1	0·0325	0·0324	0·0324	0·0324	0·0324
Rconv,2	0·0297	0·0297	0·0297	0·0297	0·0297
Rwt,1	0·0247	0·0246	0·0246	0·0246	0·0246
Rwt,2	0·0238	0·0238	0·0238	0·0238	0·0238

* Models: (1) All Mg in $T(1)$. (2) All Mg in $M(1)$. (3) Total tetrahedral site cations = 1·00. (4) Total tetrahedral site cations ~0·5 × total octahedral cations. (5) Mg in $T(1)$ = 0·5 × Mg in $M(1)$.

† Rconv, is conventional R, 1 all reflections, 2 less reflections with zero intensity. Rwt is weighted R, 1 all reflections, 2 less reflections with zero intensity.

Final positional and thermal parameters are given in Table 1.* The isotropic extinction parameter for type I extinction, Lorentzian distribution (Coppens & Hamilton, 1970), is 0·127 (20) × 10^{-4}, for refinement with anisotropic thermal parameters. Weak residual density peaks in the vicinity of $T(1)$, $M(1)$ and O positions, which in defect structure I were interpreted to represent local displacements of nearest- and next-nearest neighbor atoms about interstitials (Fleet, 1981*a*), were not observed in $F_o - F_c$ maps.

Discussion

The refined crystal structure of magnetite 2741 has interstitial cations in both a second tetrahedral site $T(3)$, equipoint position 48(f), and a second octahedral site $M(2)$, equipoint 96(h) (Fig. 2). The $T(2)$ site, partially occupied in defect structure I, is vacant to within the limits of resolution of the present refinement technique. Thus the defect structure of magnetite 2741 is basically different from that of magnetite 633 (structure I), and it therefore seems appropriate to refer to it as defect structure II. Total tetrahedral and octahedral site cations are, respectively, 0·993 (16) and 1·990 (26) per formula unit (Table 3). The defect concentration is appreciably greater than that of structure I and therefore the complementary $T(1)$ and $M(1)$ site vacancies [0·069 (14) and 0·047 (13), respectively] are well resolved. The $M(2)$ site cations are in sixfold clusters about equipoint position 16(c) (Fig. 2), being slightly displaced from 16(c) coordinates in a manner which increases $M(2)$–$T(1)$ and $M(2)$–$T(3)$ distances and decreases $M(2)$–$M(1)$ distances. Local displacements of nearest-neighbor and next nearest-neighbor cations equivalent to those reported for structure I were not resolved in the refinement. Nevertheless such accommodations are

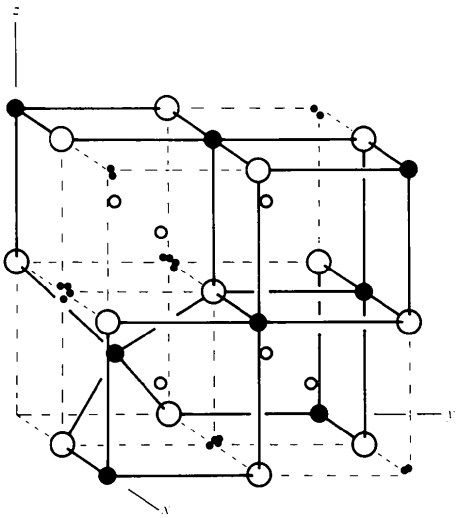

Fig. 2. Crystal structure of magnetite 2741 (defect structure II) within x = 0 to ½, y = 0 to ½, z = 0 to ½, showing location of $T(3)$ interstitials (small open circle) and $M(2)$ interstitials [small closed circles adjacent to equipoint 16(c)].

* A list of structure factors has been deposited with the British Library Lending Division as Supplementary Publication No. SUP 36735 (2 pp.). Copies may be obtained through The Executive Secretary, International Union of Crystallography, 5 Abbey Square, Chester CH1 2HU, England.

required to increase the interstitial-oxygen bond distances closer to the equilibrium values.

The present refinement of the crystal structure of magnetite 2741 thus confirms the earlier conclusion (Fleet, 1981*a*) that natural magnetite has a defect structure. The residual electron density which has been identified with the presence of interstitial cations is unlikely to be an artifact of the structure refinement for the following reasons: (1) the $T(3)$ and $M(2)$ site occupancies refine to values which are consistent with electron density peaks in $F_o - F_c$ maps *and* with corresponding vacancies in $T(1)$ and $M(1)$ positions; (2) there is a striking improvement in the refinement when the point defects are included in the structure: the weighted R decreases from 0·036 to 0·024; (3) $M(2)$ site cations are displaced from ideal 16(*c*) coordinates and the $M(2)$ positional parameter is refinable. Clearly the residual electron density in question represents structural features. There remains the possibility that these (features) may be associated with a complexly twinned structure. Incoherent twinning may be eliminated by the failure to detect twin-related reflections. Since the apparent defect concentration is about 5%, such reflections would be observed quite readily. Coherent twinning or stacking faults have already been discounted as a cause of the $\langle 110 \rangle^*$ diffuse diffraction streaks because they seem to be energetically unfavorable. However, the most persuasive argument negating such interpretations of the residual electron density is that the $M(2)$ equipoint position, which is displaced from 16(*c*) coordinates, cannot be derived from $M(1)$ by simple fractional translations. Thus in any hypothetical nonperiodic coherently twinned (or dislocated) structure the defects would have to be restricted to the twin composition (or stacking fault) planes, which would require for the high concentration of defects observed a seemingly prohibitively high density of structural domains.

The ideal inverse-spinel component of the crystal structure of magnetite 2741 is virtually identical to that of magnetite 633 (Table 1) and the earlier conclusions (Fleet, 1981*a*) on the stereochemistry of the $T(1)$ and $M(1)$ cation sites and electron configuration of $M(1)$ cations are unchanged.

The proposed defect structure of magnetite 2741 is an average structure. Short-range ordering is not resolved but stereochemical considerations argue in favor of interstitial-vacancy coupling. The good agreement between the total tetrahedral and octahedral cations and the ideal magnetite formula $Fe(T)Fe(M)_2O_4$ suggests that the conventional tetrahedral/octahedral site preferences have been observed in forming cation interstitials. Discussion of the possible effects of point defects, in the concentrations reported for defect structures I and II, on the solid-state properties of magnetite will be made elsewhere. Subsequent studies will include high-resolution X-ray structure refinement of pure and doped synthetic magnetite.

I thank H. C. Palmer for demagnetization experiments and R. L. Barnett for the electron microprobe analysis. This study was supported by a Natural Sciences and Engineering Research Council of Canada operating grant.

References

COPPENS, P. & HAMILTON, W. C. (1970). *Acta Cryst.* A**26**, 71–83.

FLEET, M. E. (1976). *J. Appl. Cryst.* **9**, 190–192.

FLEET, M. E. (1981*a*). *Acta Cryst.* B**37**, 917–920.

FLEET, M. E. (1981*b*). *Phys. Chem. Miner.* **7**, 64–70.

International Tables for X-ray Crystallography (1974). Vol. IV. Birmingham: Kynoch Press.

KRIESSMAN, C. J. & HARRISON, S. E. (1956). *Phys. Rev.* **103**, 857–860.

LINDSLEY, D. H. (1976). *Short Course Notes*, **3**, edited by D. RUMBLE III, Vol. 3, pp. L-1–L-61. New York: Mineralogical Society of America.

MACKIN, J. H. (1968). *Ore Deposits of the United States*, 1933–1967, Vol. II, edited by J. D. RIDGE, pp. 992–1019. New York: American Institute of Mining, Metallurgical and Petroleum Engineers.

OSBORNE, M. D., FLEET, M. E. & BANCROFT, G. M. (1981). *Contrib. Mineral. Petrol.* **77**, 251–255.

ROTH, W. L. (1960). *Acta Cryst.* **13**, 140–149.

SAMUELSEN, E. J. (1974). *J. Phys. C*, **7**, L115–L117.

SINKANKAS, J. (1964). *Mineralogy: A First Course.* Princeton, New Jersey: Van Nostrand.